Iris Recognition System using LBP and Linear SVC

Mahesha Y.
Associate Professor,
Department of CSE, MRIT,
Mandya, Karnataka, India

ABSTRACT
In this paper, experiment has been conducted to find the optimum iris recognition system between the combinations Local Binary Pattern (LBP) and Distance metric, and LBP and Linear Support Vector Classifier (SVC). First, experiment has been conducted using LBP and different distance metrics. For each of the distance metric, the FAR, FRR and accuracy have been calculated for different threshold values. From the obtained result, it has been found that cityblock distance gives better accuracy compared to remaining distance metrics and the accuracy obtained is 65.93% on CASIA iris dataset. Secondly, iris recognition has been carried out using Local Binary Pattern (LBP) and Linear Support Vector Classifier (SVC). The combination of LBP and Linear SVC is giving an accuracy of 91.83% on CASIA iris dataset.

Keywords
Local Binary Patterns, Linear SVC, FAR, FRR, Accuracy

1. INTRODUCTION
Biometric recognition refers to the study of identifying persons based on their unique physical traits or behavioral characteristics [1]. Physical characteristics commonly include an iris, face, fingerprint, retina, vein, voice or hand geometry, while behavioral characteristics may include handwriting, walking gait, signature, and typing keystrokes. To be useful a biometric requires features that can be accurately analysed to provide unique and stable information about a person that can be used reliably in authentication applications and many advances have been made in this area [2]. The iris has easily accessible and unique features that are stable over the lifetime of an individual. For this reason, iris recognition technology has been widely studied in the field of information security [3]. Iris recognition systems can already be applied to identify individuals in controlled access and security zones, and could feasibly be used for verification of passengers at immigration, airports, stations, computer access at research organization, database access control in distributed systems etc. [4]. Iris recognition systems can also be applied in the field of financial services such as banking services and credit card use, and such a system would not have the same vulnerabilities as passwords and numbers. Iris recognition systems are being trialled in many countries for national ID cards, immigration, national border control, airline crews, airport staffs, and missing children identification etc. [4]. While there are still some concerns about using iris-based recognition in mass consumer applications due to iris data capturing issues, it is widely believed that, in time, the technology is likely to find its way into common use [5]. Figure 1 shows different components of an eye.

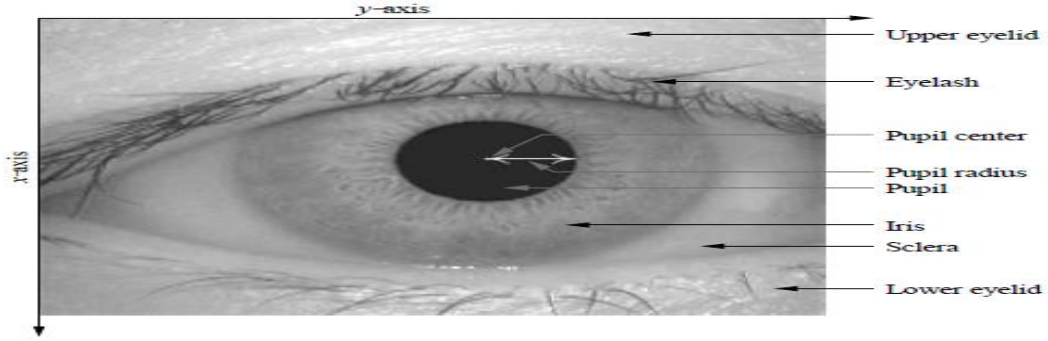

Figure 1: Components of an Eye image

In the present paper, iris verification has been done on the selected dataset. The experiment has been conducted on iris recognition using LBP and various distance metrics. Also, iris recognition has been carried out using LBP and Linear SVC.

2. MATERIALS AND METHODS
Iris images used for conducting experiment have been taken from CASIA database. First, pre-processing is done on iris images. After pre-processing, normalized iris images are obtained. Next, iris has been conducted using two different approaches. The methods used for conducting experiments are explained below.

Pre-Processing
In this research, segmentation process was carried out in several stages, namely median blur filter [6], thresholding and canny filter [7]. Initial data processing aims to process the image for obtaining the characteristics of the image so as to gain more accurate information. The results of the step sequence in the initial processing of the data are shown in Figure (2).

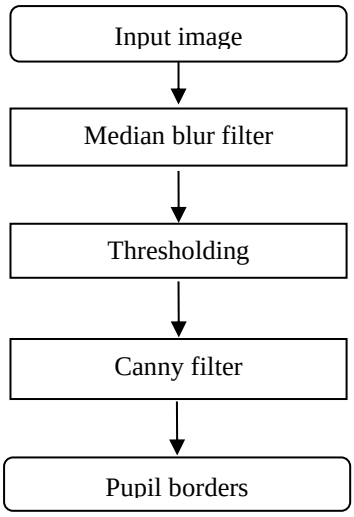

Figure 2: Pre-Processing steps

Median blur filter

In median filter, run through the signal entry by entry, replacing each entry with the median of neighboring entries. The pattern of neighbours is called the "window", which slides, entry by entry, over the entire signal. For one-dimensional signals, the most obvious window is just the first few preceding and following entries, whereas for two-dimensional (or higher-dimensional) data the window must include all entries within a given radius or ellipsoidal region.

Thresholding

Thresholding is a type of image segmentation, where we change the pixels of an image to make the image easier to analyze. In thresholding, we convert an image from color or grayscale into a binary image, i.e., one that is simply black and white. Most frequently, we use thresholding as a way to select areas of interest of an image, while ignoring the parts we are not concerned with.

Canny filter

It is a multi-stage algorithm. These steps are explained below.

1. Noise Reduction
Remove the noise in the image with a 5x5 Gaussian filter

2. Finding Intensity Gradient of the Image
Smoothened image is then filtered with a Sobel kernel in both horizontal and vertical direction to get first derivative in horizontal direction (Gx) and vertical direction (Gy). From these two images, we can find edge gradient and direction for each pixel as given in Eq. 1 and Eq. 2.

$$Edge\_Gradient(G) = \sqrt{G_x^2 + G_y^2} \quad (1)$$

$$Angle(\theta) = tan^{-1}(\frac{G_y}{G_x}) \quad (2)$$

Gradient direction is always perpendicular to edges. It is rounded to one of four angles representing vertical, horizontal and two diagonal directions.

3. Non-maximum Suppression
After getting gradient magnitude and direction, a full scan of image is done to remove any unwanted pixels which may not constitute the edge. For this, at every pixel, pixel is checked if it is a local maximum in its neighborhood in the direction of gradient.

4. Hysteresis Thresholding
This stage decides which are all edges are really edges and which are not. For this, we need two threshold values, minVal and maxVal. Any edges with intensity gradient more than maxVal are sure to be edges and those below minVal are sure to be non-edges, so discarded. Those who lie between these two thresholds are classified edges or non-edges based on their connectivity. If they are connected to "sure-edge" pixels, they are considered to be part of edges. Otherwise, they are also discarded.

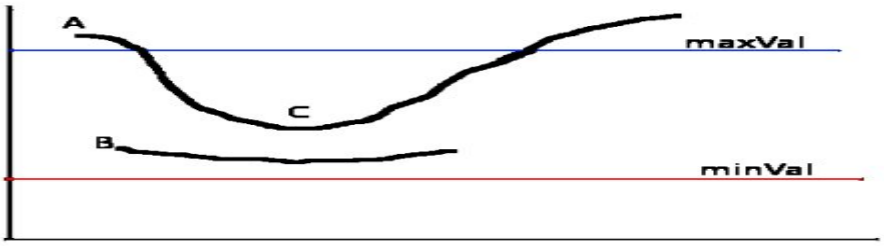

Figure 3: Hysteresis Thresholding

In Figure 3, the edge A is above the maxVal, so considered as "sure-edge". Although edge C is below maxVal, it is connected to edge A, so that also considered as valid edge and we get that full curve. But edge B, although it is above minVal and is in same region as that of edge C, it is not connected to any "sure-edge", so that is discarded. So it is very important that we have to select minVal and maxVal accordingly to get the correct result.

Iris recognition using LBP and Linear SVC

In iris recognition, the normalized iris images have been taken as input to Local Binary Pattern (LBP) [8,9]. The LBP irises haven divided into training and testing set. The Liner Support Vector Classifier (SVC) has been used to train the system for iris identification. After training, the accuracy of the system is calculated using test images. The steps involved in iris identification are shown in Figure 4. The steps involved in LBP and Liner SVC are explained below.

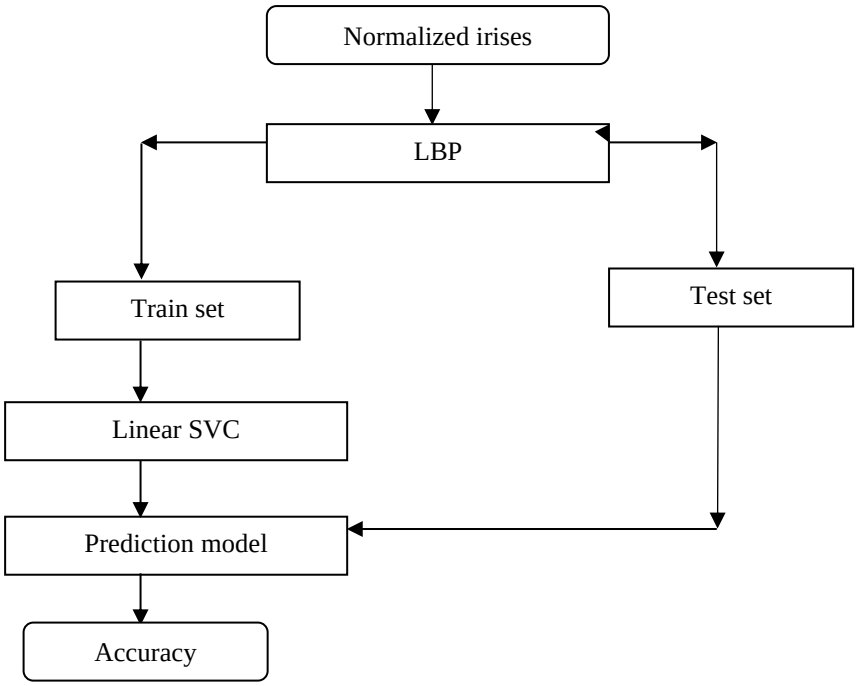

Figure 4: LBP and Linear SVC

Local Binary Pattern (LBP)

As shown in Figure 5, the LBP operator is computed for the center pixel by comparing the intensity value of it with the intensity values of its neighbours [10,11].

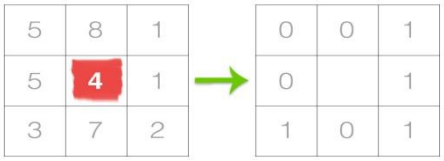

Figure 5: LBP operation

This process can be expressed mathematically as shown in Eq. 3.

$LBP_{P,R} = \sum_{p=0}^{p=1} 2^p s(i_p - i_c)$, s(x)=1 if x>=0 and s(x)=0 if x<0 (3)

Where i_c and i_p denote the gray value of the center pixel and gray value of the neighbor pixel on a circle of radius , respectively, and is the number of the neighbors. Bilinear interpolation estimation method is used to estimate the neighbors that do not lie exactly in the center of the pixels. $LBP_{P,R}^{ri}$ and $LBP_{P,R}^{riu2}$ are rotation invariant of LBP and uniform rotation invariant of LBP, respectively [12]. These two enhanced LBP operators are proposed by Ojala et al. [23]. After completing the encoding step for any LBP operators, that is, $LBP_{P,R}^{ri}$ and $LBP_{P,R}^{riu2}$ the histogram can be created based on the Eq. 4.

$H(k) = \sum\sum f(LBP_{P,R}(i,j),k), k\varepsilon[0,K]$ f(x,y)=1 if x=y, f(x,y)=0 otherwise (4)

Where k is the maximal LBP pattern value. The encoding LBP is shown in Figure 6.

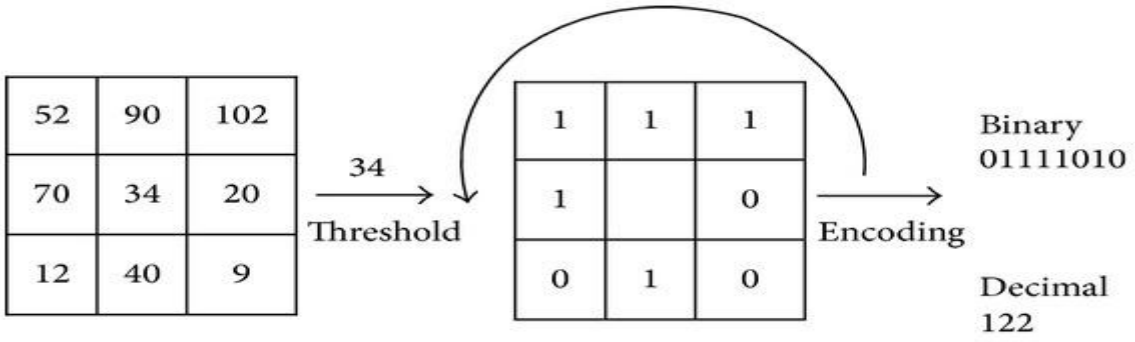

Figure 6: LBP operator

Liner Support Vector Classifier (SVC)

The linear support vector classifier can be represented by the Eq. 5 [13,14,15].

$f(x) = \beta_0 + \sum_{i=1}^{n} \alpha_i < x, x_i >$ (5)

To estimate the parameters α_1, α_2, α_3 ..... α_n and β_0 all we need are the $\binom{n}{2}$ inner products $< x_i, x_i^{'} >$between all pairs of training observations

It turns out that most of the $\hat{\alpha_i}$ can be zero

$$f(x) = \beta_0 + \sum_{i \varepsilon S}^{n} \hat{\alpha_i} < x, x_i > \quad (6)$$

S is the support set of indices i such that $\hat{\alpha_i} > 0$

Iris Recognition using LBP and Distance metrics

In iris recognition, the normalized iris images have been taken as input. The signature for each iris images has been generated using Two Dimensional Discrete Wavelet Transform. Seven different distance metrics have been applied to find the distance between signatures of iris images. The False Rejection Rate, False Acceptance Rate and Equal Error Rate have calculated for each of the distance metric. The different steps involved in iris verification is shown in Figure 7.

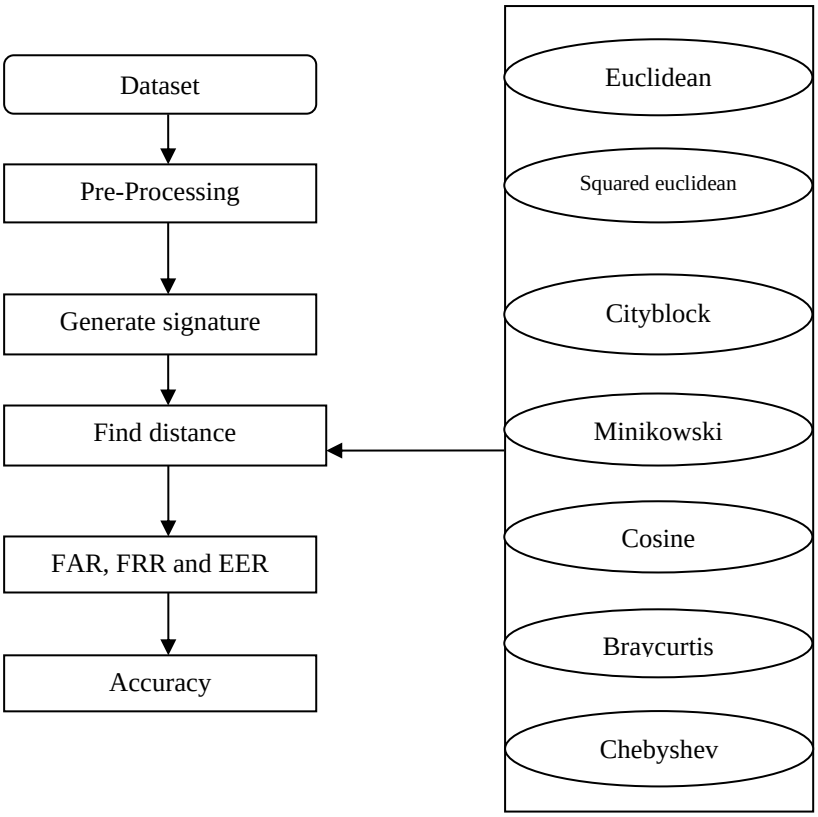

Figure 7: LBP and Distance metrics

The different distance metrics used for finding the dissimilarity between the signatures generated by the LBP are explained below.

Euclidean distance

The Euclidean distance between 1-D arrays *u* and *v*, is defined as given in Eq. (7) [16].

$$(\sum(w_i|(u_i - v_i)|^2))^{1/2} \quad (7)$$

Squared Euclidean distance

The squared Euclidean distance between *u* and *v* is defined as given in Eq. (8) [17].

$$(\sum(w_i|(u_i - v_i)|^2)) \quad (8)$$

Cityblock distance

Computes the Manhattan distance between two 1-D arrays *u* and *v*, which is defined as given in Eq. (9). [18,19]

$$\sum_i |u_i - v_i| \quad (9)$$

Minkowski distance

The Minkowski distance between 1-D arrays *u* and *v*, is defined as given in Eq. (10)[20,21].

$$(\sum w_i(|\,(u_i - v_i)|^p))^{1/p} \quad (10)$$

Cosine distance

The Cosine distance between *u* and *v*, is defined as given in Eq. (12) [22,23].

$$1 - \frac{u \bullet v}{||u||_2||v_2||} \quad (12)$$

Bray-Curtis distance

Bray-Curtis distance is defined as given in Eq. (13) [24,25]

$$\sum |u_i - v_i| / \sum |u_i + v_i| \quad (13)$$

Chebyshev distance

Computes the Chebyshev distance between two 1-D arrays *u* and *v*, which is defined as given in Eq. (14) [26,27].

$$\max_i |u_i - v_i| \quad (14)$$

Evaluation and validation of experimental results

To evaluate some distance measurement methods, this study used several measurements as follows:

1. False Rejected Rate (FRR): False Rejected Rate (FRR) indicates a system error in which the system rejects the input data that the system should accept [28]. FRR is calculated using the Eq. 15.

$$FRR = \frac{NFR}{NAA} * 100 \quad (15)$$

Where, NFR (Number of False Rejection) is the number of event when system incorrectly rejects the data. NAA (Number of Authentic Attempt) is the total number of events.

2. False Acceptance Rate (FAR): FAR indicates a system error in which accepts the input data that the system should reject [28]. FAR is calculated using the Eq. (*).

$$FAR = \frac{NFA}{NUA} * 100 \quad (16)$$

Where, NFA (Number of False Acceptance) is the number of event when system incorrectly rejects the data. NUA (Number of Unauthentic Attempt) is the total number of events.

3. Accuracy: The accuracy is calculated using the Eq. 17 [28].

$$Accuracy = 100 - [(FAR + FRR)/2] \quad (17)$$

3. RESULTS AND DISCUSSION

Pre-Processing

The iris images used for the study are taken from CASIA database. The iris image has to pass through pre-processing stage. In pre-processing stage, the thresholded image is obtained from the original image as in Figure 8.

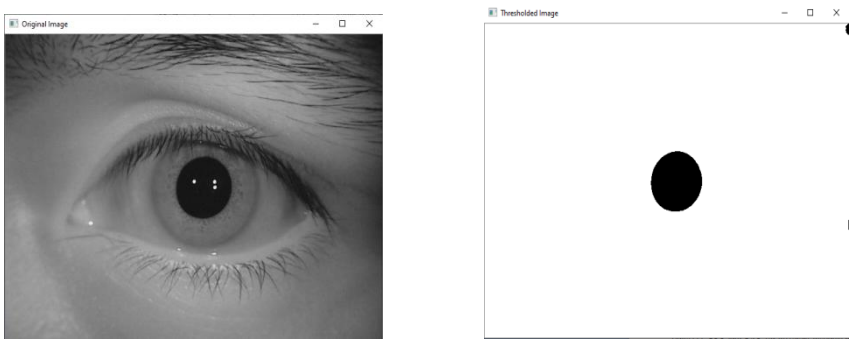

(a) (b)

Figure 8: (a) Original image (b) Thresholded image

The normalized iris image has been obtained as shown in Figure 9.

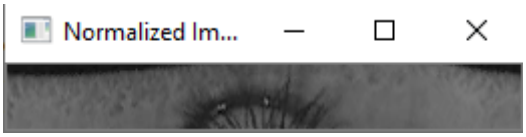

Figure 9: Normalized iris

The difference or dissimilarity between signatures is obtained using seven distance metrics. The False Rejection Rate (FRR) and False Acceptance rate (FAR) for different distance metrics are given in Table (*).

Iris recognition using LBP and Distance metrics

Table 1 shows the FAR and FRR at the threshold obtained at EER

Table 1: FRR and FAR for different distance metrics

Euclidean		Squared euclidean		Cityblock		Minkowski		Cosine		Braycurtis		Chebyshev	
FAR	**FRR**	**FAR**	**FRR**	**FAR**	**FRR**	**FAR**	**FRR**	**FAR**	**FRR**	**FAR**	**FRR**	**FAR**	**FRR**
34.89	37.46	61.90	13.56	33.24	34.89	34.89	37.56	72.52	10.07	37.31	31.46	38.14	36.14

Table 2 shows the FAR and FRR at different threshold values

Table 2: FAR and FRR at different threshold values

Euclidean			Squared Euclidean		Cityblock		Minkowski		Cosine		Braycurtis		Cheybyshev	
T	FRR	FAR	FRR	FAR	FRR	FAR	FRR	FAR	FRR	FAR	FRR	FAR	FRR	FAR
0.00	100	0.00	100	0.00	100	0.00	100	0.00	100	0.00	100	0.00	100	0.00
0.01	99.91	0.00	13.56	61.90	100	0.00	99.91	0.00	10.07	72.52	100	0.00	94.78	0.92
0.02	92.49	0.89	6.15	80.12	100	0.00	92.49	0.89	4.68	87.83	99.85	0.00	76.12	9.63
0.03	76.85	6.62	4.12	88.85	100	0.00	76.85	6.62	3.77	93.52	96.40	0.18	60.10	20.72
0.04	62.00	15.97	3.00	93.49	99.85	0.00	62.00	15.97	3.01	96.18	86.94	1.70	46.54	30.20
0.05	48.08	25.86	2.33	96.08	98.87	0.02	48.08	25.86	2.21	97.43	74.52	5.94	36.14	38.13
0.06	37.45	34.89	1.91	97.55	96.40	0.18	37.45	34.89	2.00	98.01	61.47	12.75	27.92	45.24
0.07	30.00	42.77	1.67	98.38	92.14	0.68	30.00	42.77	1.75	98.29	49.29	20.78	21.64	51.87
0.08	23.17	49.84	1.47	98.89	86.94	1.70	23.17	49.84	1.63	98.52	38.92	29.12	16.45	58.04
0.09	17.80	56.17	1.22	99.21	80.94	3.45	17.80	56.17	1.52	98.75	31.45	37.31	12.42	63.82
0.10	13.56	61.90	0.98	99.43	74.52	5.94	13.56	61.90	1.38	98.97	24.57	44.82	9.54	68.97
0.11	10.42	67.08	0.80	99.59	67.89	9.08	10.42	67.08	1.21	99.19	19.22	51.79	7.78	73.61
0.12	8.49	71.74	0.56	99.71	61.47	12.75	8.49	71.74	0.98	99.37	15.07	57.98	6.33	77.77
0.13	7.14	75.90	0.40	99.81	55.05	16.63	7.14	75.90	0.73	99.54	11.71	63.55	5.29	81.38
0.14	6..24	79.64	0.17	99.88	49.29	20.78	6.24	79.64	0.50	99.68	9.56	68.52	4.56	84.56
0.15	5.31	82.89	0.07	99.93	43.89	24.96	5.31	82.89	0.42	99.80	8.10	72.83	4.01	87.28
0.16	4.75	85.72	0.07	99.95	38.92	29.12	4.75	85.72	0.22	99.87	7.03	76.75	3.42	89.60
0.17	-	-	-	-	34.89	33.24	-	-	-	-	-	-	-	-
-	-	-	-	-	-	-	-	-	-	-	-	-	-	-

The accuracy of each distance metric is given in the Table 3.

Table 3: Accuracy

Distance metric	Accuracy (%)
Cityblock	65.93
Braycurtis	65.61
Euclidean	63.82
Chebychev	62.86
Minkowski	63.77
Squared Euclidean	62.27
Cosine	58.70

ROC curve has been drawn for each of the distance metric as shown in Figure 10. The Equal Error Rate has been obtained from the graph.

FRR: 37.46 FAR:34.89

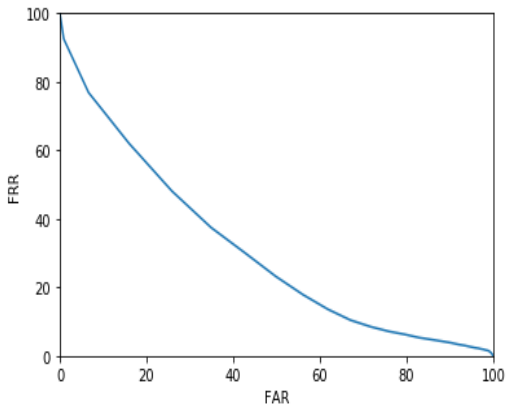

(a) Euclidean

FRR: 13.56 FAR:61.90

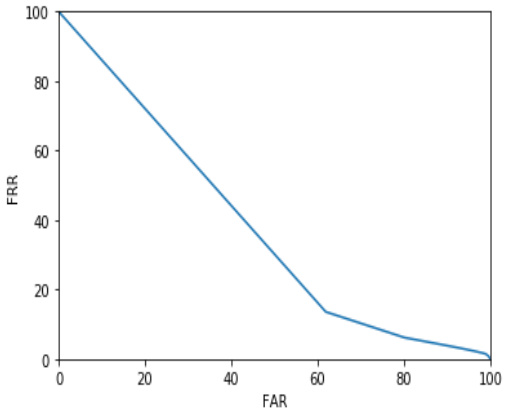

(b) Squared Euclidean

FRR: 34.89 FAR: 33.24

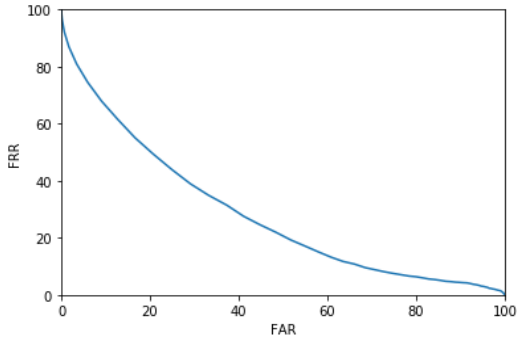

(c) Cityblock

FRR: 37.46 FAR: 34.89

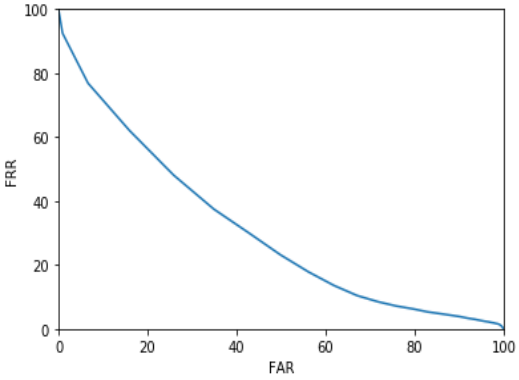

(d) Minkowski

FRR: 10.07 FAR: 72.52

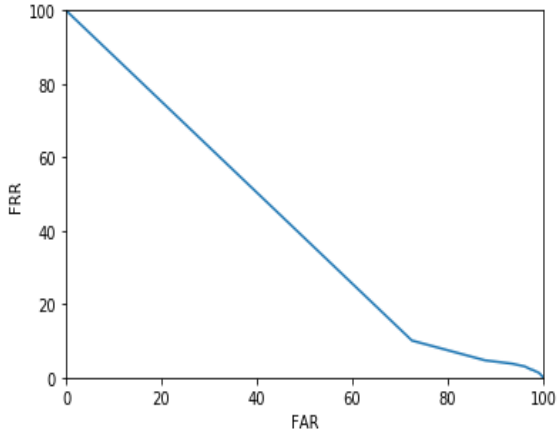

(e) Cosine

FRR: 31.46 FAR:37.31

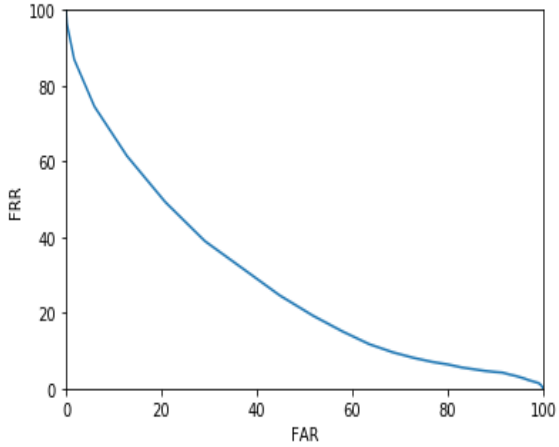

(f) Braycurtis

FRR: 36.14 FAR: 38.14

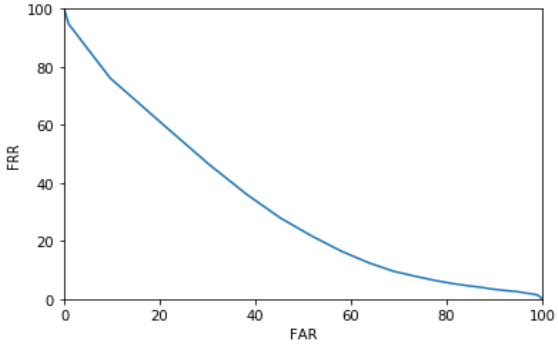

(g) Chebyshev

Figure 10: FAR and FRR for different distance metrics

The graph has been plotted to show the FAR, FRR and Accuracy for different distance metrics as shown in Figure 11.

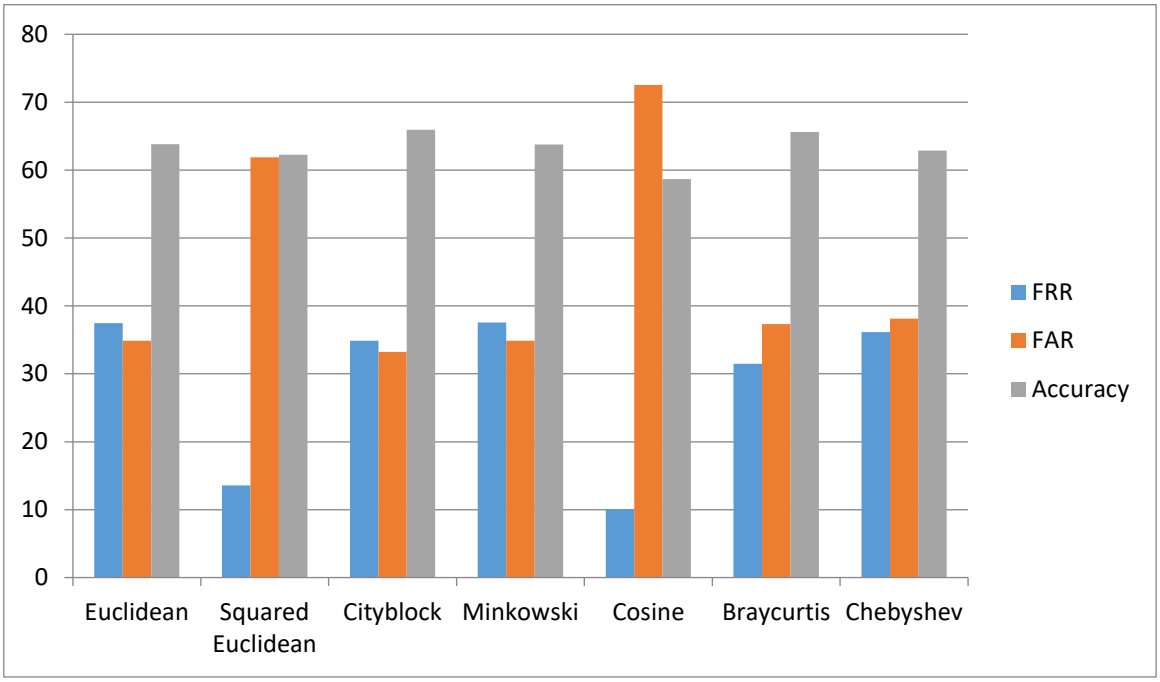

Figure 11: FRR, FAR and Accuracy for different distance metrics

Iris identification using LBP and Linear SVM

The Local Binary Pattern has been applied on normalized image. The LBP image is shown in Figure 12. The Linear Support Vector Classifier has been used to develop a prediction model. The accuracy of the developed system has been tested. The experiment has been conducted ten times and in each time different train and test have been used. Mean value of accuracy is calculated along with standard deviation and they are listed in Table (*).

Figure 12: LBP image

From the CASIA database, 150 images have been used as train set and remaining 300 images have been taken as test set. The LBP for all the training examples has been generated and prediction model has been developed using the SVM. The Table 3 shows the FAR and FRR values. The False Rejection Rate (FRR), False Acceptance Rate (FAR) and Accuracy are calculated using the Eq. (18), Eq. (19) and Eq. (20) respectively.

$$FRR = \frac{NFR}{NAA} * 100 \quad (18)$$

$$FAR = \frac{NFA}{NIA} * 100 \quad (19)$$

$$Accuracy = 100 - (FRR + FAR) \quad (20)$$

Table 3: FRR, FAR and Accuracy

NFR	NAA	NFA	NIA	FRR	FAR	Accuracy
4	150	3	150	2.67 %	2.00 %	95.33 %

NAA-Number of Authenticated Attempts, NIA- Number of Imposter Attempts, NFR- Number of False Rejections, NFA-Number of False Acceptance

The accuracy of iris identification obtained is 91.83%. The Table 4 shows the accuracy obtained from the combination LBP and Linear SVC, and LBP and city block distance.

Table 4: Accuracy for different combinations

Method	Accuaracy (%)
LBP and Linear SVC	91.83
LBP and Cityblock distance	65.93

4. CONCLUSION

The present research work conducted experiment to find the optimum iris recognition between the combinations LBP and Linear SVC, and LBP and distance metric with the help of CASIA iris dataset. First, iris recognition has been done using LBP and seven distance metrics such as Euclidean, Squared Euclidean, Cityblock, Minkowski, Cosine, Braycurtis and Chebyshev. The FAR, FRR and Accuracy have been calculated for each of the distance metric. Among these seven distance metrics, cityblock distance has shown better accuracy compared to remaining six distance metrics and the achieved accuracy is 65.93%. Secondly, iris recognition has been

conducted using the combination LBP and Linear SVC. This combination is achieving an accuracy of 91.83%. Among the combinations LBP and Distance metrics, and LBP and Linear SVC, the LBP and Linear SVC is achieving better accuracy.

5. REFERENCES

[1] A fast iris recognition system through optimum feature extractionRana HK, Azam MS, Akhtar MR, Quinn JMW, Moni MA. 2019. A fast irisrecognition system through optimum feature extraction. PeerJ ComputerScience 5:e184 https://doi.org/10.7717/peerj-cs.184

[2] Naseem, I., Aleem, A., Togneri, R., and Bennamoun, M. (2017). Iris recognition using class-specificdictionaries. Computers & Electrical Engineering, 62:178–193.

[3] Umer, S., Dhara, B. C., and Chanda, B. (2017). A novel cancelable iris recognition system based on feature learning techniques. Information Sciences, 406:102–118.

[4] Galdi, C., Nappi, M., and Dugelay, J.-L. (2016). Multimodal authentication on smartphones: Com- bining iris and sensor recognition for a double check of user identity. Pattern Recognition Letters,222 82:144–153.

[5] Nabti, M. and Bouridane, A. (2008). An effective and fast iris recognition system based on acombined multiscale feature extraction technique. Pattern recognition, 41(3):868–879.

[6] G J Yang and T S Huang. (1981). The effect of median filtering on edge location estimation. Computer graphics and Image processing, 15(3): 224-245.

[7] Chiluka Nagaraju and I Raja sekhar Reddy (2016). Canny scale edge detection. International Journal of Engineering Trends and Technology (IJETT).

[8] Li Liu, Lingjun Zhao, Yunli Long, Gangyao Kuang and Paul Fieguth. 2012. Extended local binary patterns for texture classification. Image and Vision Computing, 30(2):86-99.

[9] Loris Nanni, Alessandra Lumini and Sheryl Brahnam. 2010. Local binary patterns variants as texture descriptors for medical image analysis. Artificial Intelligence in Medicine, 49(2): 117-125.

[10] SONG Ke-Chen1 YAN Yun-Hui1 CHEN Wen-Hui1 ZHANG Xu1, Research and Perspective on Local Binary Pattern. Acta Automatica Sinica, 39(6): 731-745.

[11] Timo Ahonen, Abdenour Hadid and Matti Pietikainen, Face recognition with Local Binary Pattern. European Conference on Computer Vision, 469-481.

[12] Di Huang, Caifeng Shan, Mohsen Ardebilian, Yunhong Wang and Liming Chen. Local Binary Patterns and Its Application to Facial Image Analysis: A Survey, IEEE Transactions on Systems, Man, and Cybernetics, Part C (Applications and Reviews), 41(6), 765-781.

[13] Lubor Ladicky and Philip H S Torr. 2011. Locally Linear Support Vector Machines, International Conference on Machine Learning, Bellevue, WA, USA.

[14] Chunhua Zhanga , Xiaojian Shaob and Dewei Lia. 2015. Knowledge-based Support Vector Classification Based on C-SVC. Information Technology and Quantitative Management. 1083-1090.

[15] Chia-Hua Ho and Chih-Jen Lin. 2012. Large-scale Linear Support Vector Regression. Journal of Machine Learning Research. 3323-3348.

[16] Leo Liberti, Carlile Lavor, Nelson Maculan and Antonio Mucherino. 2012. Quantitative methods. arXiv:1205.0349.

[17] Dokmanic, R. Parhizkar, J. Ranieri and M. Vetterli, "Euclidean Distance Matrices: Essential theory, algorithms, and applications," in *IEEE Signal Processing Magazine*, vol. 32, no. 6, pp. 12-30, Nov. 2015, doi: 10.1109/MSP.2015.2398954.

[18] Y. Pan, J. L. Trahan and R. Vaidyanathan, "A Scalable and Efficient Algorithm for Computing the City Block Distance Transform on Reconfigurable Meshes," in *The Computer Journal*, vol. 40, no. 7, pp. 435-440, Jan. 1997, doi: 10.1093/comjnl/40.7.435.

[19] Mitra, Debasree & Sarkar, Parantapa & Roy, Payel. (2019). Face Recognition by City-Block Distance Classifier in Supervised Machine Learning. 10.1729/Journal.21653.

[20] Merigo, Jose M. & Casanovas, Montserrat. (2012). A New Minkowski Distance Based on Induced Aggregation Operators. International Journal of Computational Intelligence Systems. April 2011. 123-133. 10.1080/18756891.2011.9727769.

[21] Groenen, Patrick & Kaymak, Uzay & Rosmalen, J.M.. (2006). Fuzzy clustering with Minkowski distance. Erasmus University Rotterdam, Econometric Institute, Econometric Institute Report.

[22] Rahutomo, Faisal & Kitasuka, Teruaki & Aritsugi, Masayoshi. (2012). Semantic Cosine Similarity.

[23] Sitikhu, Pinky & Pahi, Kritish & Thapa, Pujan & Shakya, Subarna. (2019). A Comparison of Semantic Similarity Methods for Maximum Human Interpretability.

[24] Somerfield, Paul. (2008). Identification of the Bray-Curtis similarity index: Comment on Yoshioka (2008). Marine Ecology-progress Series - MAR ECOL-PROGR SER. 372. 303-306. 10.3354/meps07841.

[25] Edward W. 1984. Beals,Bray-Curtis Ordination: An Effective Strategy for Analysis of Multivariate Ecological Data, Editor(s): A. MacFadyen, E.D. Ford, Advances in Ecological Research, Academic Press, 14: 1-55.

[26] Coghetto, Roland. (2016). Chebyshev Distance. Formalized Mathematics. 24. 10.1515/forma-2016-0010.

[27] Kløve, Torleiv & Lin, Te-Tsung & Tsai, Shi-Chun & Tzeng, Wen-Guey. (2009). Permutation Arrays Under the Chebyshev Distance. IEEE Transactions on Information Theory. 56. 10.1109/TIT.2010.2046212.

[28] Hassan, Sabit & Shaar, Shaden & Raj, Bhiksha & Razak, Saquib. (2018). Online Evaluation of Classifier Accuracy, False Acceptance Rate and False Rejection Rate.